

See discussions, stats, and author profiles for this publication at: <https://www.researchgate.net/publication/259472693>

# Multiple Detachment of the SF<sub>6</sub><sup>-</sup> Molecular Anion with Shaped Intense Laser Pulses

ARTICLE in THE JOURNAL OF PHYSICAL CHEMISTRY A · DECEMBER 2013

Impact Factor: 2.69 · DOI: 10.1021/jp4116436 · Source: PubMed

CITATIONS

3

READS

28

## 3 AUTHORS:



Yishai Albeck

Hebrew University of Jerusalem

4 PUBLICATIONS 4 CITATIONS

SEE PROFILE



Durai Murugan

Hebrew University of Jerusalem

11 PUBLICATIONS 49 CITATIONS

SEE PROFILE



D. Strasser

Hebrew University of Jerusalem

74 PUBLICATIONS 947 CITATIONS

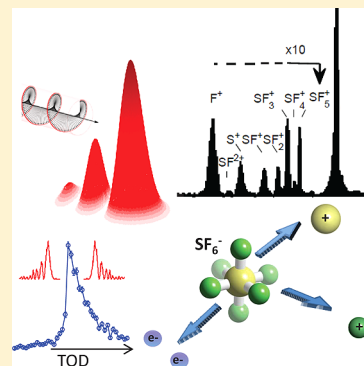
SEE PROFILE

# Multiple Detachment of the $\text{SF}_6^-$ Molecular Anion with Shaped Intense Laser Pulses

Yishai Albeck, Durai Murugan Kandhasamy, and Daniel Strasser\*

Institute of Chemistry, The Hebrew University of Jerusalem, 91904 Jerusalem, Israel

**ABSTRACT:** Interaction of molecular  $\text{SF}_6^-$  anions with intense near-IR laser pulses is found to produce cationic fragments by nonsequential multiple detachment. Dissociative ionization channels that lie more than 20 eV above the threshold energy for double detachment are observed. Mass-resolved product yields are presented and analyzed as a function of the femtosecond laser pulse energy, pulse shape, and polarization ellipticity. The observed strong suppression of multiple detachment by pre-pulses, induced with negative third-order dispersion of the transform-limited fs laser pulse, is interpreted as suppression of a nonsequential process by early single detachment. However, in contrast to the relatively simple picture of a rescattering mechanism characterized by acute sensitivity to polarization ellipticity that dominates double ionization of neutral species and was reported for the atomic  $\text{F}^-$  anion, multiple detachment of the molecular anion is found to exhibit only mild ellipticity dependence.



## 1. INTRODUCTION

The interaction of intense laser pulses with atomic and molecular matter exhibits a broad range of highly intriguing nonlinear phenomena. While processes such as multiphoton ionization (MPI) and above-threshold ionization (ATI) can often be considered perturbatively,<sup>1,2</sup> increasing laser intensities lead to double as well as multiple ionization,<sup>3–8</sup> generation of very high order harmonics (HHG),<sup>9–11</sup> and other phenomena<sup>2,6,12–14</sup> that cannot be considered perturbatively. In molecular and cluster systems, multiple ionization triggers fascinating violent events such as Coulomb explosion,<sup>6,15–17</sup> charge resonance enhanced ionization (CREI),<sup>18,19</sup> and generation of highly charged atoms.<sup>20,21</sup> Modeling double ionization dynamics and HHG in atomic matter with semiclassical approaches led to an intuitive description of rescattering dynamics that provides the foundation for attosecond science.<sup>11,22</sup> In this picture, an electron liberated by the first ionization is accelerated in the oscillating electric field of the laser and is driven back to collide with its parent ion, resulting in a second ionization event or, alternatively, a radiative recombination and emission of a high-energy photon.

Although significant progress has been made by studies of intense laser interaction with overall neutral atoms and molecules, one can expect intense field interactions with molecular anions to be significantly different from both neutral or cationic systems.<sup>23,24</sup> The typically low electron binding energies of anions make it possible to explore extreme conditions of very rapid ionization at relatively low laser intensities. In addition, significantly higher contrast can be achieved in anions between the low binding energy of the first electron and the ionization energy required to remove a second electron from the system. Furthermore, considering a rescattering mechanism, the initial wavepacket of a rescattered electron is significantly larger in the case of a loosely bound

anion, and its motion is not influenced by the long-range Coulomb attraction present in overall neutral systems.<sup>25</sup> Both experimental and theoretical efforts have been made to describe electron emission spectra from atomic anion systems in an attempt to identify evidence for the contribution of nonsequential rescattering mechanisms.<sup>23,26–29</sup> Pedregosa-Gutierrez et al. investigated the double detachment of the atomic fluorine anion, whose 3.4 eV electron affinity allows anions to survive in the ultrafast pulse and reach high enough peak intensities to produce  $\text{F}^+$  cations by a nonsequential mechanism. The authors interpreted the significant enhancement of double detachment by linearly versus circularly polarized ultrafast pulses as first evidence for a nonsequential rescattering observed in anions. In the case of molecular anion systems, nuclear motion dynamics on the excited molecular potential surfaces produced by photodetachment can lead to rich fragmentation processes. Recent experiments with  $\text{F}_2^-$  molecular anions exposed to intense laser pulses show evidence of competing electron detachment and molecular dissociation dynamics affecting the photoelectron spectrum.<sup>30</sup> To the best of our knowledge, there is no previous experimental work investigating multiple detachment of molecular anions.

In the present work, we explore intense field multiple detachment of a molecular  $\text{SF}_6^-$  anion. Double detachment of  $\text{SF}_6^-$  is expected to produce the  $\text{SF}_6^+$  system that is known to be unstable and to lead to a rich spectrum of photofragments depending on the energy provided to the system above the threshold for removing two electrons. Extensive studies of neutral  $\text{SF}_6$  dissociative ionization<sup>31–34</sup> provide us with detailed knowledge of the threshold appearance energies of the different

Received: November 27, 2013

Revised: December 22, 2013

Published: December 26, 2013



cationic products summarized in Table 1. Previous studies<sup>35</sup> of neutral  $\text{SF}_6$  ionization with intense laser pulses reported

**Table 1. Appearance Energies for the Different  $\text{SF}_6^+$  Fragmentation Products from Photoionization Experiments, Measured by Mass Spectrometry<sup>a</sup> and Electron–Ion Coincidence Measurements<sup>b</sup> along with the Corresponding Minimal Number of 800 nm Photons Needed to Reach Appearance Energy Thresholds from the Anion Ground State**

ion	AE (eV)	$N_{\text{photon}}$
$\text{F}_5\text{S}^+$	$15.3 \pm 0.2^a$	10
$\text{F}_4\text{S}^+$	$19.1 \pm 0.5^a$	13
$\text{F}_3\text{S}^+$	$19.4 \pm 0.5^a$	13
$\text{F}_2\text{S}^+$	$26 \pm 1^b$	17
$\text{FS}^+$	$31 \pm 1^b$	21
$\text{S}^+$	$37 \pm 1^b$	24
$\text{F}^+$	$38 \pm 1^b$	25

<sup>a</sup>Measured by mass spectrometry; from ref 31. <sup>b</sup>Measured by electron–ion coincidence measurements; from ref 32.

dissociative ionization yielding predominantly  $\text{SF}_5^+$  and  $\text{F}^+$  cations at peak intensities of  $4.3 \times 10^{14} \text{ W/cm}^2$  and an onset of multiple ionization at intensities above  $8 \times 10^{14} \text{ W/cm}^2$ . The adiabatic detachment energy of  $\text{SF}_6^-$  is about 1 eV.<sup>36–38</sup> However, as the additional electron increases the S–F bond length, vertical detachment of an electron from  $\text{SF}_6^-$  requires about 3 eV,<sup>37–40</sup> similar to the detachment energy of the atomic  $\text{F}^-$  anion studies,<sup>41</sup> making it a good candidate to survive as an anion and exhibit nonsequential dynamics. The bond length difference also results in the initiation of rapid nuclear wavepacket motion on the neutral  $\text{SF}_6$  ground-state surface after removal of the first electron, which may strongly influence the probability for removing an additional electron by moving the wavepacket into or away from a favorable geometry for further ionization.<sup>18,19</sup>

In the following, we show multiple detachment photo-fragmentation products of  $\text{SF}_6^-$ , including singly, doubly, and even triply charged cation species observed at peak intensities of  $4 \times 10^{13} \text{ W/cm}^2$  and above. We present cation yield dependence on pulse energy, pulse shape, and polarization

ellipticity and discuss the observed strong suppression of multiple detachment by negative third-order dispersion (TOD) and mild dependence on polarization ellipticity.

## 2. EXPERIMENTAL SETUP

In our experimental setup, shown schematically in Figure 1, cold  $\text{SF}_6^-$  anions are produced in a cold ion source, equipped with an “Even-Lavie” pulsed valve<sup>42</sup> and a 200 eV pulsed electron gun producing anions in a supersonic expansion of 300 psi of argon gas, seeded with 1% of  $\text{SF}_6$ . Anions are accelerated to 4.6 keV in a pulsed Wiley–McLaren-type time-of-flight (TOF) spectrometer, tuned to time-focus the ions at the laser–ion interaction region.<sup>43</sup> At the entrance to our home-built photofragment spectrometer, a “mass gate” deflector is grounded for  $\sim 1 \mu\text{s}$  to allow  $\text{SF}_6^-$  anions to reach the ion–laser interaction region while deflecting ions of different charge over mass ratio. After entering the photofragment spectrometer, selected ions are further accelerated by a set of eight electrodes with gradually increasing potentials from the ground potential up to 1.8 kV at the field-free laser–ion interaction region. Following the interaction region, an additional seven electrodes decelerate the parent anion beam back to the 4.6 keV beam energy, while neutral photodetachment products are not decelerated and continue traveling toward the photofragment MCP detector with the velocity of the parent ions at the interaction region. Thus, neutral photodetachment products arrive at the photofragment detector before the parent anion beam. On the other hand, cationic products of multiple detachment are further accelerated by the potential drop after the interaction region and are separated according to their charge over mass ratio, as demonstrated in the typical background-subtracted photofragment TOF spectra presented in Figure 2.

Ultrafast seed pulses are generated by a Ti-Sapphire oscillator (Mai Tai SP, Spectra-Physics, Newport Co.) centered around 800 nm. Prior to amplification in a regenerative amplifier (Spitfire pro XP, Spectra-Physics, Newport Co.), a 128 pixel computer-controlled pulse shaper (femtoJock, BioPhotonics Solutions Inc.) is used to precompensate any residual spectral phase in the amplified pulse, as well as to shape the amplified pulses by applying computer-controlled spectral phase masks.

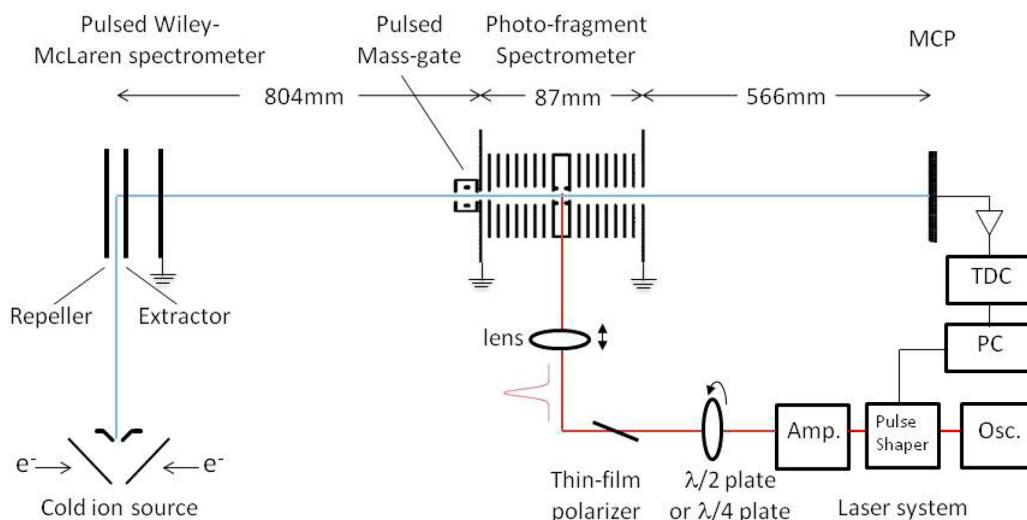


**Figure 1.** Experimental setup scheme.

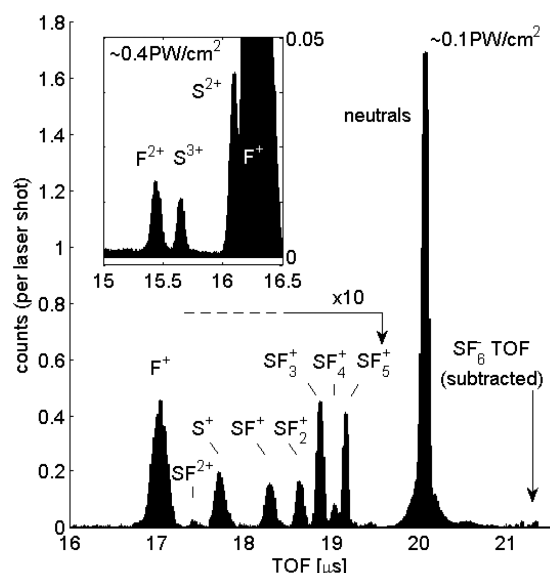


**Figure 2.** Typical background-subtracted photofragment TOF spectrum at a  $10^{14}$  W/cm<sup>2</sup> peak intensity showing single, double, and multiple detachment products. The SF<sub>6</sub><sup>+</sup> anion peak is not present, as the parent anion background is subtracted. The inset shows the multiply charged atomic cation spectra recorded at a  $4 \times 10^{14}$  W/cm<sup>2</sup> peak intensity and higher spectrometer voltage (leading to a small shift in the fragment TOF).

Pulse shaping capabilities also allow the implementation of MIIPS,<sup>44</sup> providing full phase and amplitude pulse reconstruction that is periodically performed to determine and then precompensate any residual spectral phase, assuring transform-limited amplified pulses. Typical pulses used in the experiments reported here support  $\sim 35$  fs fwhm and were typically amplified to 3.2 mJ/pulse. In addition to pulse shaping, the pulse energy and polarization ellipticity are computer-controlled without affecting the spectral phase by rotation of either a  $\lambda/2$  wave plate that is positioned in front of a broadband thin film polarizer or a  $\lambda/4$  wave plate. The laser is focused with a 250 mm focal length lens, reaching peak intensities of up to  $2.7 \times 10^{15}$  W/cm<sup>2</sup> at the  $25.5 \mu\text{m}$  wide focal volume, limited by  $M^2 \approx 1.75$ . At these conditions, the Rayleigh length is comparable to the radius of the ion beam of  $\sim 2$  mm, resulting in relatively well-defined peak intensity across the laser–anion interaction region. The actual measurements are performed with the laser focal spot displaced from the center of the anion beam to limit the peak intensity while optimizing the extent of the interaction volume. Figure 3 shows the yield of the neutral and singly and multiply charged products as a function of focal spot displacement from the interaction region and indicating the corresponding peak intensities. All charge states reach a minimum yield due to saturation of the respective process probabilities and the vanishing laser–ion overlap volume at zero displacement. On the other hand, maximal yields of neutrals and singly and multiply charged cations are respectively obtained at 12, 3.5, and 1.5 mm displacements, where the volume effect is balanced by the peak intensity dependence of the nonlinear yields. The corresponding peak intensities  $I_{\text{max}} = 0.4, 4.3, \text{ and } 15 \times 10^{14}$  W/cm<sup>2</sup> can be directly related to the saturation intensities of the different processes by  $I_{\text{sat}} = \alpha I_{\text{max}}$  where  $\alpha$  is a geometric factor with only a weak dependence on the nonlinear order of each process and laser beam shape. Numerical estimates considering a Gaussian beam

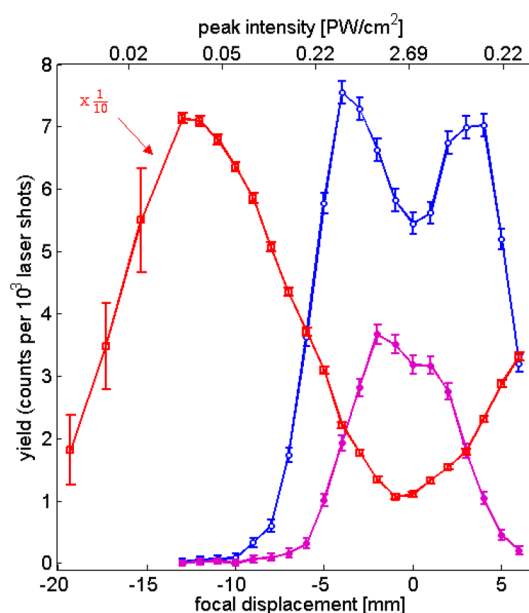


**Figure 3.** A focus scan profile of the different photodetachment products: neutral SF<sub>6</sub> (squares), cations (empty circles), and multiply ionized fragments (full circles). The maxima relate to the balance between the intensity and volume considerations and occur at different focal displacements of 12, 3.5, and 1.5 mm, corresponding to intensities of 0.4, 4.3, and  $15 \times 10^{14}$  W/cm<sup>2</sup> for neutral and singly and multiply ionized products, respectively.

profile and a realistic finite ion beam show that the geometric factor is rapidly converging from  $\alpha \approx 0.5$  for second-order intensity dependence to  $\alpha \approx 0.4$  for orders greater than 4. In order to characterize the effects of pulse shaping and polarization ellipticity on the double and multiple detachment mechanisms while avoiding saturation of said processes, measurements were performed at 7.5 mm displacement from the focal point, corresponding to maximal peak intensities of  $10^{14}$  W/cm<sup>2</sup>.

### 3. RESULTS AND DISCUSSION

**Photofragment Spectrum.** Figure 2 shows typical photofragmentation TOF spectra obtained for SF<sub>6</sub><sup>−</sup> ions irradiated by pulses reaching peak intensities of  $10^{14}$  W/cm<sup>2</sup> (the figure inset showing a spectrum collected at a  $4.3 \times 10^{14}$  W/cm<sup>2</sup> peak intensity). The most dominant peak arriving 1.1  $\mu\text{s}$  before the parent anions (anions not shown) corresponds to neutral products, predominantly due to photodetachment of a single electron, although other dissociative channels also contribute neutral products arriving at the same time. The earlier peaks, arriving at descending TOF order, correspond to SF<sub>5</sub><sup>+</sup>, SF<sub>4</sub><sup>+</sup>, SF<sub>3</sub><sup>+</sup>, SF<sub>2</sub><sup>+</sup>, SF<sup>+</sup>, S<sup>+</sup>, and F<sup>+</sup> singly charged cationic fragments that are resolved according to their charge over mass ratio. SF<sub>6</sub><sup>+</sup> is known to be unstable<sup>45</sup> and is not observed, and similarly, the lower yield of SF<sub>4</sub><sup>+</sup> compared to SF<sub>5</sub><sup>+</sup> and SF<sub>3</sub><sup>+</sup> is in accord with its lower stability.<sup>32</sup> Interestingly, although the appearance energy of fully dissociated atomic S<sup>+</sup> and F<sup>+</sup> lies more than 37 eV above the neutral SF<sub>6</sub> ground state, the atomic species dominate the cation spectrum at peak intensities higher than  $5 \times 10^{14}$  W/cm<sup>2</sup>, as will be discussed in the following. Higher charge state products due to multiple detachment are also observed; the 17.4  $\mu\text{s}$  peak can be tentatively assigned to a stable molecular SF<sub>2</sub><sup>2+</sup> dication, and for higher peak intensities,

shown in the figure inset, multiply ionized atomic products of  $S^{2+}$ ,  $F^{2+}$ , and even  $S^{3+}$  are clearly observed.

Further insight can be drawn from coincidence analysis of the TOF data shown in Figure 4. The strong  $F^+-SF_n^+$

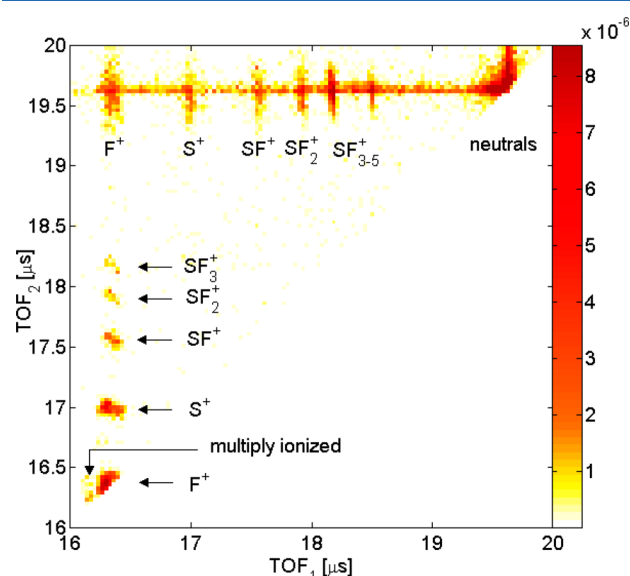


**Figure 4.** Photofragment coincidence analysis. The color scale represents the probability of fragments arriving in coincidence at  $TOF_1$  and at  $TOF_2$  after a single laser shot.

correlation signals indicate the strong contribution of Coulomb explosion of multiply ionized unstable molecular cations to the observed cation spectra. In fact, it is clear that the observed atomic  $S^+$  and  $F^+$  cations are predominantly dissociation products of multiply ionized intermediate species. On the other hand, molecular cations are more likely to form by double detachment followed by dissociation of the unstable  $SF_6^+$  parent cation. For example, one can note that for both  $SF_5^+$  and  $SF_3^+$ , coincidence is more than an order of magnitude higher with neutral compared to cationic products. One can also note the TOF width of the atomic peaks, indicating a significant kinetic energy release along the TOF axis, characteristic of the Coulombic explosion of the multiply charged parent molecule. SIMION ion trajectory simulations, taking into account the experimental geometry and the exact photofragment spectrometer potentials, indicate that the observed TOF widths corresponds to a kinetic energy release of  $\sim 5$  eV in the observed  $F^+-S^+$  coincidences. Interestingly, similar TOF widths are observed for laser polarization parallel or perpendicular to the TOF axis, indicating relatively isotropic photofragment emission and detection efficiency.

**Pulse Energy Dependence.** Figure 5 shows the cation yield dependence on pulse energy that is varied by changing the overall laser pulse energy while maintaining a fixed pulse length. Measurements are performed at a 7.5 mm ion beam displacement from the laser focus, corresponding to peak intensities of  $10^{14}$  W/cm $^2$  and lower, well below the saturation of cation production. A simple  $I^n$  power law dependence successfully describes the data with a power of  $n = 3.6 \pm 0.2$  and  $2.6 \pm 0.3$  for the production of fully dissociated atomic and molecular cations, respectively, with a crossing of atomic and molecular dominance that is reached at a peak intensity of  $5 \times 10^{13}$  W/cm $^2$ . The observed power dependence is significantly lower than the minimal number of 800 nm photons required to

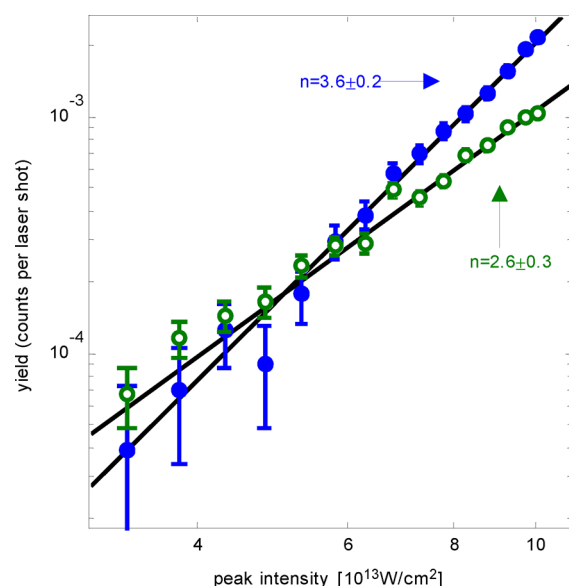


**Figure 5.** Cation yields measured as a function of pulse energy. Full circles represent the atomic fragment yield, while empty circles represent the molecular fragment yield. Lines represent power law fits to the data with  $n = 3.6 \pm 0.2$  and  $2.6 \pm 0.3$  for atomic and molecular cation fragment yields, respectively.

reach the appearance energies of these photoproducts, as indicated in Table 1, suggesting enhancement either by resonances or by an efficient nonsequential process such as the rescattering mechanism for double ionization of neutral species. Although direct comparison is difficult to make, we note that multiple ionization is observed at  $3 \times 10^{14}$  W/cm $^2$  peak intensities that are lower than the intensities at which multiple ionization of neutral  $SF_6$  was studied.<sup>35,46</sup> The observed power dependence is also weak compared to tunnel-ionization of argon atoms, having an ionization potential comparable to the appearance energies of  $SF_5^+$  but exhibiting an  $n \approx 6$  power law in the same peak intensity regime.<sup>47</sup> Separate measurements of neutral yield power dependence, conducted at weaker focusing and peak intensities below  $1.6 \times 10^{13}$  W/cm $^2$ , resulted in a power dependence of  $n = 2$ , in agreement with the minimal number of near-IR photons needed to reach the vertical detachment energy of  $SF_6^-$ .

**Pulse Shaping Experiments.** By applying an appropriate spectral phase, we can examine how multiple detachment of electrons from molecular anions depends on the shape of the pulse. Figure 6 shows the change in the yield of cations as a function of chirp applied to the pulse, which stretches the 35 fs pulses in time and consequently lowers their peak intensity while keeping the pulse energy fixed. We present the combined singly charged cation yield as both the molecular and singly charged atomic cations showed the same trend within the experimental error bars. Chirp dependence is found to be relatively weak, similar to the surprisingly weak dependence on pulse energy. Although slightly higher efficiency is observed for long positively versus negatively chirped pulses, the overall chirp response is symmetric with respect to the direction of the frequency chirp and compatible with a nonresonant mechanism that does not depend strongly on the ordering of frequencies within the stretched pulses from low to high frequencies or vice versa.

With the advent of a versatile pulse shaper control of the spectral phase, we can also stretch the pulses in time by



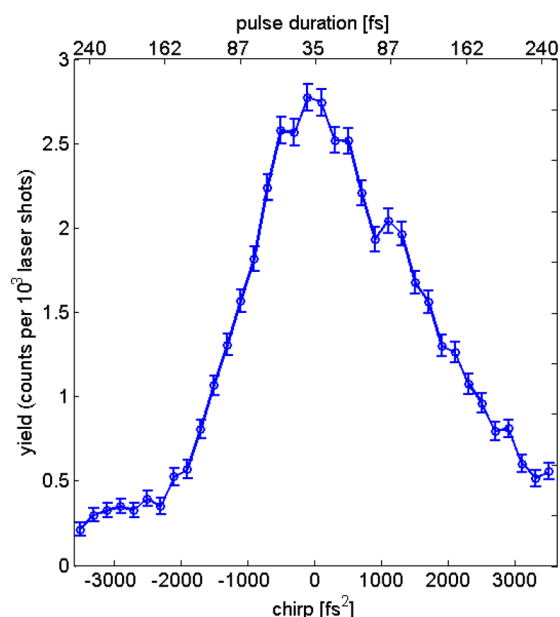


Figure 6. Cation yield as a function of chirp applied to the pulse.

applying TOD to the pulse, which leads to pulses that are asymmetric in time rather than in frequency. For negative TOD pulses, the central part of the spectrum is delayed with respect to the high- and low-frequency parts, resulting in beating pre-pulses followed by a main intense pulse. On the other hand, by applying positive TOD, we delay the high- and low-frequency tails of the spectrum, resulting in a main short pulse followed by beating post-pulses. Figure 7 shows the measured cation yields as a function of TOD applied to the pulse, as well as typical pulse shapes, calculated based on our MIIPS measurements. The data clearly show higher yields for pulse shapes with a sharp rising pulse followed by post-pulses, compared to slowly rising pre-pulses ending in an intense pulse.

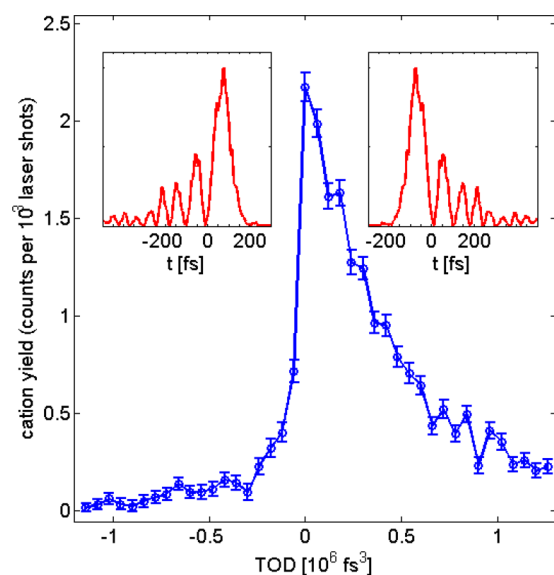
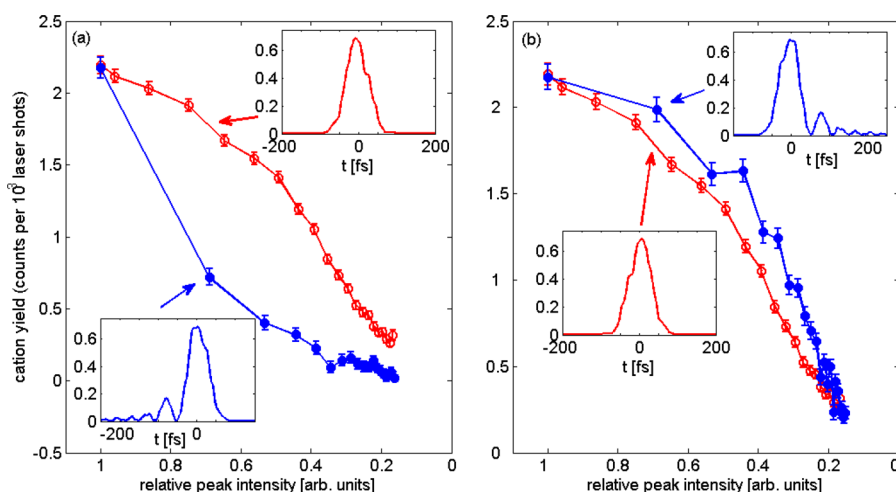


Figure 7. The TOD scan profile of the singly ionized products. A pronounced asymmetric trend is observed with a higher signal for positive TOD relative to negative, corresponding to a post- and pre-pulsed asymmetric pulse (in the insets for  $\text{TOD} = \pm 3 \times 10^5 \text{ fs}^{-3}$ ).

As both chirp and TOD scans are conducted simultaneously, alternating the computer-controlled spectral phases every 20 s and keeping all other experimental conditions fixed, it is insightful to directly compare the actual cation yields obtained with chirped and TOD pulses at comparable peak intensities. The full circles in Figure 8a and b show the cation yields obtained with positive and negative TOD, respectively, while the empty circles in both panels show the average yields obtained with positive and negative chirps and the same peak intensity. While positive TOD induces a mild response similar to the observed response to chirp and pulse energy variation, negative TOD is found to strongly suppress the multiple detachment mechanism. Even a relatively small change in peak intensity that leads to a mild  $\sim 10\%$  reduction in cation yield when induced by chirp or positive TOD leads to a strong  $\sim 70\%$  suppression for negative TOD pulses. Weak pre-pulses may in some cases enhance the interaction with intense laser pulses by aligning molecular rotations<sup>48</sup> or Raman exciting vibrational modes, as was demonstrated for enhancement of HHG in neutral  $\text{SF}_6$  molecules by properly timed pre-pulses.<sup>49</sup> However, we observe a rapid suppression with applied negative TOD and not an enhancement at an optimal pre-pulse beating frequency. We also observe that the relatively weak pre-pulses have peak intensities reaching  $\sim 1.5 \times 10^{13} \text{ W/cm}^2$ , comparable with the saturation intensity that we derived for production of neutrals by single detachment. We therefore propose that a non-sequential multiple detachment mechanism is suppressed by efficient single detachment prior to the arrival of the intense pulse, in contrast to a sequential mechanism that can be expected to be enhanced by such pre-pulses. Along the same line of thought, the energy of two near-IR photons is closer to the  $\text{SF}_6^-$  vertical detachment energy for the blue tail of our spectrum, leading possibly to a higher probability for two-photon detachment by the rising edge of long negatively chirped pulses. Consequently, we can speculate that early detachment also accounts for the slight asymmetry observed for long chirped pulses, as shown in Figure 6.

We conclude that the observed cation production is facilitated by the weakly bound electron of the anion and that multiple detachment of the  $\text{SF}_6^-$  molecular anion is governed by a nonsequential process. In the following, we explore the possibility of a recollision mechanism, similar to the dominant mechanism for double ionization of neutral species.

**Polarization Ellipticity Dependence.** Nonsequential double ionization of neutral atoms and molecules is typically dominated by rescattering mechanisms.<sup>5,50,51</sup> As rescattering is driven by the oscillating electric field of the laser pulse, these types of mechanisms are dramatically sensitive to the ellipticity of the laser pulse polarization. At these field intensities, polarized light drives a classical electron nanometers away from its original position, clearly missing the molecule and strongly suppressing rescattering mechanisms. Even slight ellipticity of 0.2 steers the accelerated electron away from its parent ion and efficiently suppresses any recollision mechanism.<sup>52</sup> Figure 9 shows the yield of cations as a function of ellipticity at a constant pulse energy. Although a cation yield with circularly polarized pulses is 40% lower compared to the yield obtained with linear polarization, the drop is observed to be gradual as a function of ellipticity, contrary to what can be expected from a rescattering-type mechanism. Such ellipticity dependence could perhaps reflect the gradual decrease of the maximal electric field strength, changing by a factor of the square root of 2 between linear and circular polarizations. It is important to note that



**Figure 8.** Comparing the chirp scan (empty circles) with the TOD scan (full circles), as attenuation of peak intensity, for both (a) negative and (b) positive phases. In the insets are examples of pulse intensity profiles with the TOD ( $\pm 10^4$  fs<sup>3</sup>) and with the chirp ( $\pm 350$  fs<sup>2</sup>). All intensities are normalized to the peak intensity of a transform-limited pulse.

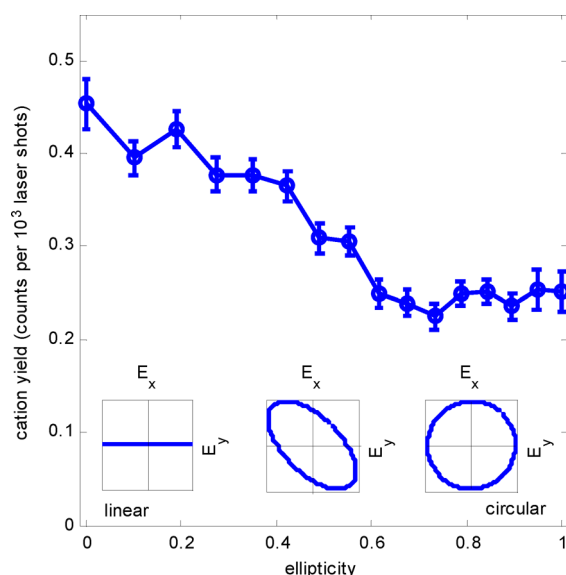


**Figure 9.** The results of an ellipticity scan, tuned from linear to circular polarization of the laser, showing little dependence on the ellipticity.

within the experimental error bars, we observe no significant change in the photofragment spectra between linear and circular polarizations, supporting the assumption of similar multiple detachment mechanisms at both polarization conditions. On the other hand, Pedregosa-Gutierrez et al. did report significant enhancement of double ionization of atomic F<sup>−</sup> with linearly polarized compared to circularly polarized light and interpreted this observation as evidence for a nonsequential multiple detachment via a rescattering mechanism, observed at peak intensities of  $\sim 2 \times 10^{14}$  W/cm<sup>2</sup>, comparable to the intensities used in the present study. It is possible that the extended wave function of a molecular anion leads to a different response to ellipticity from the dramatic suppression predicted by a simple semiclassical rescattering picture and observed in double ionization of neutral species.<sup>11,52</sup> Alternatively, different mechanisms may dominate nonsequential multiple detachment in atomic and molecular anion systems.

#### 4. CONCLUSIONS

In conclusion, neutral and cationic photofragment spectra of the molecular SF<sub>6</sub><sup>−</sup> anion detachment by intense laser pulses were recorded as a function of pulse energy, pulse shape, and polarization ellipticity. Cationic, multiple detachment products of SF<sub>6</sub><sup>−</sup> were observed at peak intensities as low as  $4 \times 10^{13}$  W/cm<sup>2</sup>. On the basis of the measured balance between the volume effect and nonlinear intensity dependence, saturation intensities of 0.16, 1.7, and  $6 \times 10^{14}$  W/cm<sup>2</sup> were derived for the respective production of neutral, singly charged, and multiply charged cations. Comparing pulses stretched by chirp and TOD with equal peak intensities alludes to a nonsequential mechanism, which is quenched by the pre-pulses caused by negative TOD that detach the loosely bound electron prior to the arrival of the main pulse. The strong sensitivity to TOD, which is rarely controlled even in state of the art intense field experiments, can help explain the difficulty reported in previous attempts to observe nonsequential multiple detachment of anions by intense fields.<sup>23,27</sup> Finally, we find that for the SF<sub>6</sub><sup>−</sup> molecular anion, the gradual and smooth dependence of multiple detachment on the polarization ellipticity does not fit a simple picture of a rescattering mechanism. Other mechanisms of multielectron dynamics will be required to account for the multiple detachment of the molecular SF<sub>6</sub><sup>−</sup> anion. The typically higher polarizability of anions compared to their neutral counterparts and the distortion of the octahedral SF<sub>6</sub> structure by the additional electron<sup>38</sup> may perhaps lead to stronger anion–laser interaction and account for the observed pre-pulse suppression,<sup>53</sup> without the need for invoking an ellipticity-sensitive semiclassical rescattering mechanism. However, further theoretical and experimental investigations are required to better describe intense field interactions with molecular anions.

#### AUTHOR INFORMATION

##### Notes

The authors declare no competing financial interest.

##### ACKNOWLEDGMENTS

The authors gratefully acknowledge funding from the European Community's seventh frame work [FP7/2007-2013] under

Grant Agreement #247471, as well as from the Legacy Heritage fund (Israel Science Foundation). We also acknowledge the assistance of Prof. Ori Cheshnovsky of Tel-Aviv University who provided us with the cold ion source system as well as valuable knowhow.

## REFERENCES

- (1) Mainfray, G.; Manus, C. Multiphoton Ionization of Atoms. *Rep. Prog. Phys.* **1991**, *54*, 1333–1372.
- (2) Posthumus, J. The Dynamics of Small Molecules in Intense Laser Fields. *Rep. Prog. Phys.* **2004**, *67*, 623–665.
- (3) L'Huillier, A.; Lompre, L.; Mainfray, G.; Manus, C. Multiply Charged Ions Induced by Multiphoton Absorption in Rare Gases at 0.53  $\mu\text{m}$ . *Phys. Rev. A* **1983**, *27*, 2503–2512.
- (4) Walker, B.; Mevel, E.; Yang, B.; Breger, P.; Chambaret, J.; Antonetti, A.; Dimauro, L.; Agostini, P. Double Ionization in the Perturbative and Tunneling Regimes. *Phys. Rev. A* **1993**, *48*, 894–897.
- (5) Rudenko, A.; Zrost, K.; Feuerstein, B.; de Jesus, V.; Schröter, C.; Moshhammer, R.; Ullrich, J. Correlated Multielectron Dynamics in Ultrafast Laser Pulse Interactions with Atoms. *Phys. Rev. Lett.* **2004**, *93*, 253001.
- (6) Sheehy, B.; DiMauro, L. F. Atomic and Molecular Dynamics in Intense Optical Fields. *Annu. Rev. Phys. Chem.* **1996**, *47*, 463–494.
- (7) Lezius, M.; Blanchet, V.; Ivanov, M. Y.; Stolow, A. Polyatomic Molecules in Strong Laser Fields: Nonadiabatic Multielectron Dynamics. *J. Chem. Phys.* **2002**, *117*, 1575–1588.
- (8) Dörner, R.; Weber, Th.; Weckenbrock, M.; Staudte, A.; Hattass, M.; Schmidt-Bocking, H.; Moshhammer, R.; Ullrich, J. Multiple Ionization in Strong Laser Fields. *Adv. At. Mol. Opt. Phys.* **2002**, *48*, 1–34.
- (9) Paul, P. M.; Toma, E. S.; Breger, P.; Mullot, G.; Auge, F.; Balcou, Ph.; Muller, H. G.; Agostini, P. Observation of a Train of Attosecond Pulses from High Harmonic Generation. *Science* **2001**, *292*, 1689–1692.
- (10) Seres, J.; Seres, E.; Verhoef, A. J.; Tempea, G.; Strelli, C.; Wobruschek, P.; Yakovlev, V.; Scrinzi, A.; Spielmann, C.; Krausz, F. Source of Coherent Kilo-electronvolt X-rays. *Nature* **2005**, *433*, 596.
- (11) Corkum, P. B. Plasma Perspective on Strong Field Multiphoton Ionization. *Phys. Rev. Lett.* **1993**, *71*, 1994–1997.
- (12) Roudnev, V.; Esry, B.; Ben-Itzhak, I. Controlling  $\text{HD}^+$  and  $\text{H}_2^+$  Dissociation with the Carrier-Envelope Phase Difference of an Intense Ultrashort Laser Pulse. *Phys. Rev. Lett.* **2004**, *93*, 163601.
- (13) Sussman, B. J.; Townsend, D.; Ivanov, M. Y.; Stolow, A. Dynamic Stark Control of Photochemical Processes. *Science* **2006**, *314*, 278–281.
- (14) Boguslavskiy, A. E.; Mikosch, J.; Gijbbersen, A.; Spanner, M.; Patchkovskii, S.; Gador, N.; Vrakking, M. J. J.; Stolow, A. The Multielectron Ionization Dynamics Underlying Attosecond Strong-Field Spectroscopies. *Science* **2012**, *335*, 1336–1340.
- (15) Sattler, K.; Mühlbach, J.; Echt, O.; Pfau, P.; Recknagel, E. Evidence for Coulomb Explosion of Doubly Charged Microclusters. *Phys. Rev. Lett.* **1981**, *47*, 160–163.
- (16) Ivanov, M.; Seideman, T.; Corkum, P. B.; Ilkov, F.; Dietrich, P. Explosive Ionization of Molecules in Intense Laser Fields. *Phys. Rev. A* **1996**, *54*, 1541–1550.
- (17) Pitzer, M.; Kunitzki, M.; Johnson, A. S.; Jahnke, T.; Sann, H.; Sturm, F.; Schmidt, L. P. H.; Schmidt-Böcking, H.; Dörner, R.; Stohner, J.; et al. Direct Determination of Absolute Molecular Stereochemistry in Gas Phase by Coulomb Explosion Imaging. *Science* **2013**, *341*, 1096–1100.
- (18) Zuo, T.; Bandrauk, A. D. Charge-Resonance-Enhanced Ionization of Diatomic Molecular Ions by Intense Lasers. *Phys. Rev. A* **1995**, *52*, 2511–2514.
- (19) Bocharova, I.; Karimi, R.; Penka, E. F.; Brichta, J. P.; Lassonde, P.; Fu, X.; Kieffer, J. C.; Bandrauk, A. D.; Litvinyuk, I.; Sanderson, J.; et al. Charge Resonance Enhanced Ionization of  $\text{CO}_2$  Probed by Laser Coulomb Explosion Imaging. *Phys. Rev. Lett.* **2011**, *107*, 063201.
- (20) Snyder, E. M.; Buzza, S. A.; Castleman, A. W., Jr. Intense Field–Matter Interactions: Multiple Ionization of Clusters. *Phys. Rev. Lett.* **1996**, *77*, 3347–3350.
- (21) Ditmire, T.; Tisch, J. W. G.; Springate, E.; Mason, M. B.; Hay, N.; Smith, R. A.; Marangos, J.; Hutchinson, M. H. R. High-Energy Ions Produced in Explosions of Superheated Atomic Clusters. *Nature* **1997**, *386*, 54–56.
- (22) Corkum, P. B.; Krausz, F. Attosecond Science. *Nat. Phys.* **2007**, *3*, 381–387.
- (23) Kiyan, I. Y.; Helm, H. Production of Energetic Electrons in the Process of Photodetachment of  $\text{F}^-$ . *Phys. Rev. Lett.* **2003**, *90*, 183001.
- (24) Pedregosa-Gutierrez, J.; Orr, P. A.; Greenwood, J. B.; Murphy, A.; Costello, J. T.; Zrost, K.; Ergler, T.; Moshhammer, R.; Ullrich, J. Evidence for Rescattering in Intense, Femtosecond Laser Interactions with a Negative Ion. *Phys. Rev. Lett.* **2004**, *93*, 223001.
- (25) Bhardwaj, V. R.; Aseyev, S. A.; Mehendale, M.; Yudin, G. L.; Villeneuve, D. M.; Rayner, D. M.; Ivanov, M. Y.; Corkum, P. B. Few Cycle Dynamics of Multiphoton Double Ionization. *Phys. Rev. Lett.* **2001**, *86*, 3522–3525.
- (26) Greenwood, J. B.; Collins, G. F.; Pedregosa-Gutierrez, J.; McKenna, J.; Murphy, A.; Costello, J. T. Double Ionization of Atomic Negative Ions in an Intense Laser Field. *J. Phys. B: At. Mol. Opt. Phys.* **2003**, *36*, L235–L240.
- (27) Reichle, R.; Helm, H.; Kiyan, I. Y. Detailed Comparison of Theory and Experiment of Strong-Field Photodetachment of the Negative Hydrogen Ion. *Phys. Rev. A* **2003**, *68*, 063404.
- (28) Bergues, B.; Kiyan, I. Y. Two-Electron Photodetachment of Negative Ions in a Strong Laser Field. *Phys. Rev. Lett.* **2008**, *100*, 143004.
- (29) Gazibegović-Busuladžić, A.; Milošević, D. B.; Becker, W.; Bergues, B.; Hultgren, H.; Kiyan, I. Y. Electron Rescattering in Above-Threshold Photodetachment of Negative Ions. *Phys. Rev. Lett.* **2010**, *104*, 103004.
- (30) Hultgren, H.; Kiyan, I. Y. Photodetachment Dynamics of  $\text{F}_2^-$  in a Strong Laser Field. *Phys. Rev. A* **2011**, *84*, 015401.
- (31) Sasanuma, M.; Ishiguro, E.; Hayaisha, T.; Masuko, H.; Morioka, Y.; Nakajima, T.; Nakamura, M. Photoionisation of  $\text{SF}_6$  in the XUV Region. *J. Phys. B: At. Mol. Opt. Phys.* **2001**, *34*, 4057–4063.
- (32) Hitchcock, A.; Van der Wiel, M. J. Absolute Oscillator Strengths (5–63 eV) for Photoabsorption and Ionic Fragmentation of  $\text{SF}_6$ . *J. Phys. B: At. Mol. Opt. Phys.* **1979**, *12*, 2153–2169.
- (33) Feifel, R.; Eland, J. H. D.; Storch, L.; Tarantelli, F. Complete Valence Double Photoionization of  $\text{SF}_6$ . *J. Chem. Phys.* **2005**, *122*, 144309.
- (34) Christophorou, L. G.; Olthoff, J. K. Electron Interactions with  $\text{SF}_6$ . *J. Phys. Chem. Ref. Data* **2000**, *29*, 267–330.
- (35) Sanderson, J.; Thomas, R.; Bryan, W.; Newall, W.; Taday, P.; Langley, A. Multielectron-Dissociative-Ionization of  $\text{SF}_6$  by Intense Femtosecond Laser Pulses. *J. Phys. B: At. Mol. Opt. Phys.* **1997**, *30*, 4499–4507.
- (36) Troe, J.; Miller, T. M.; Viggiano, A. A. Communication: Revised Electron Affinity of  $\text{SF}_6$  from Kinetic Data. *J. Chem. Phys.* **2012**, *136*, 121102.
- (37) Gutsev, G. L.; Barlett, R. J. Adiabatic Electron Affinities of  $\text{PF}_5$  and  $\text{SF}_6$ : A Coupled-Cluster Study. *Mol. Phys.* **1998**, *94*, 121–125.
- (38) Eisfeld, W. Highly Accurate Determination of the Electron Affinity of  $\text{SF}_6$  and Analysis of Structure and Photodetachment Spectrum of  $\text{SF}_6^-$ . *J. Chem. Phys.* **2011**, *134*, 054303.
- (39) Datskos, P. G.; Carter, J. G.; Christophorou, L. G. Photodetachment of  $\text{SF}_6^-$ . *Chem. Phys. Lett.* **1995**, *239*, 38–43.
- (40) Bopp, J. C.; Roscioli, J. R.; Johnson, M. A.; Miller, T. M.; Viggiano, A. A.; Villano, S. M.; Wren, S. W.; Lineberger, W. C. Spectroscopic Characterization of the Isolated  $\text{SF}_6^-$  and  $\text{C}_4\text{F}_8^-$  Anions: Observation of Very Long Harmonic Progressions in Symmetric Deformation Modes Upon Photodetachment. *J. Phys. Chem. A* **2007**, *111*, 1214–1221.
- (41) Andersen, T.; Haugen, H. K.; Hotop, H. Binding Energies in Atomic Negative Ions: III. *J. Phys. Chem. Ref. Data* **1999**, *28*, 1511–1533.



- (42) Luria, K.; Lavie, N.; Even, U. Dielectric Barrier Discharge Source for Supersonic Beams. *Rev. Sci. Instrum.* **2009**, *80*, 104102.
- (43) Wiley, W. C.; McLaren, I. H. Time-of-Flight Mass Spectrometer with Improved Resolution. *Rev. Sci. Instrum.* **1955**, *26*, 1150–1157.
- (44) Lozovoy, V. V.; Pastirk, I.; Dantus, M. Multiphoton Intrapulse Interference. IV. Ultrashort Laser Pulse Spectral Phase Characterization and Compensation. *Opt. Lett.* **2004**, *29*, 775–777.
- (45) Hitchcock, A. P.; Brion, C. E.; Van der Wiel, M. J. Ionic Fragmentation of SF<sub>6</sub> Ionised in the Sulphur 2p Shell. *J. Phys. B: At. Mol. Opt. Phys.* **1978**, *11*, 3245–3261.
- (46) Ren, H.; Ma, R.; Li, X.; Chen, J.; Yang, H.; Gong, Q. Multielectron Dissociative Ionization of SF<sub>6</sub> in an Intense Femto-second Laser Field. *Int. J. Mass Spectrom.* **2004**, *235*, 117–122.
- (47) Larochelle, S.; Talebpour, A.; Chin, S. L. Non-Sequential Multiple Ionization of Rare Gas Atoms in a Ti: Sapphire Laser Field. *J. Phys. B: At. Mol. Opt. Phys.* **1998**, *31*, 1201, 1215–1224.
- (48) Velotta, R.; Hay, N.; Mason, M. B.; Castillejo, M.; Marangos, J. P. High-Order Harmonic Generation in Aligned Molecules. *Phys. Rev. Lett.* **2001**, *87*, 183901.
- (49) Wagner, N. L.; Wüest, A.; Christov, I. P.; Popmintchev, T.; Zhou, X.; Murnane, M. M.; Kapteyn, H. C. Monitoring Molecular Dynamics Using Coherent Electrons from High Harmonic Generation. *Proc. Natl. Acad. Sci. U.S.A.* **2006**, *103*, 13279–13285.
- (50) Gillen, G. D.; Walker, M. A.; Van Woerkom, L. D. Enhanced Double Ionization with Circularly Polarized Light. *Phys. Rev. A* **2001**, *64*, 043413.
- (51) Weber, Th.; Weckenbrock, M.; Staudte, A.; Spielberger, L.; Jagutzki, O.; Mergel, V.; Afaneh, F.; Urbasch, G.; Vollmer, M.; Giessen, H.; et al. Recoil-Ion Momentum Distributions for Single and Double Ionization of Helium in Strong Laser Fields. *Phys. Rev. Lett.* **2000**, *84*, 443–446.
- (52) Dietrich, P.; Burnett, N. H.; Ivanov, M.; Corkum, P. B. High-Harmonic Generation and Correlated Two-Electron Multiphoton Ionization with Elliptically Polarized Light. *Phys. Rev. A* **1994**, *50*, 3585–3588.
- (53) Markevitch, A. N.; Romanov, D. A.; Smith, S. M.; Schlegel, H. B.; Ivanov, M. Y.; Levis, R. J. Sequential Nonadiabatic Excitation of Large Molecules and Ions Driven by Strong Laser Fields. *Phys. Rev. A* **2004**, *69*, 013401.